AD-A122 446 MBE IN MOS TECHNOLOGY APPLIED TO SPEED INCREASES IN VHSICS(U) VARIAN ASSOCIATES INC PALO ALTO CA T J MALONEY SEP 82 N00014-81-C-2598 1/1

UNCLASSIFIED F/G 20/8 NL

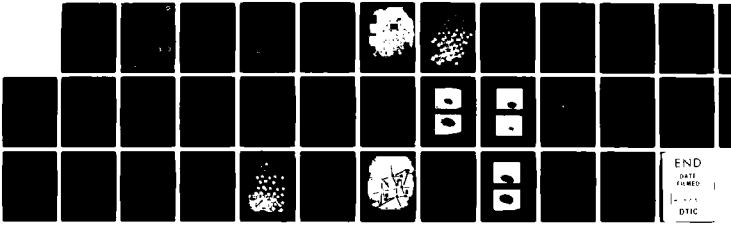

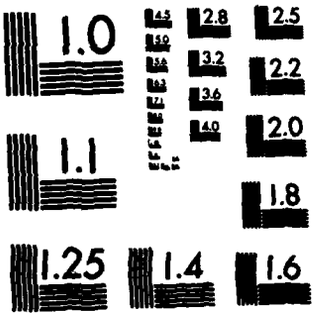

12

MBE IN MOS TECHNOLOGY APPLIED TO SPEED INCREASES IN VHSICs

FINAL REPORT

Contract N00014-81-C-2598

September 1982

Prepared for:

Naval Research Laboratory
Washington, DC 20395

Prepared by:

Timothy J. Maloney

Varian Associates, Inc.
Solid State Laboratory
Palo Alto, CA 94303

UNCLASSIFIED

SECURITY CLASSIFICATION OF THIS PAGE (When Data Entered)

REPORT DOCUMENTATION PAGE	READ INSTRUCTIONS BEFORE COMPLETING FORM
1. REPORT NUMBER	2. GOVT ACCESSION NO. AD-A122446	3. RECIPIENT'S CATALOG NUMBER
4. TITLE (and Subtitle) MBE in MOS Technology Applied to Speed Increases in VHSICs	5. TYPE OF REPORT & PERIOD COVERED Final Report Sept. 1981 -- Sept. 1982
	6. PERFORMING ORG. REPORT NUMBER
7. AUTHOR(s) Timothy J. Maloney	8. CONTRACT OR GRANT NUMBER(s) N00014-81-C-2598
9. PERFORMING ORGANIZATION NAME AND ADDRESS Varian Associates, Inc. 611 Hansen Way Palo Alto, CA 94303	10. PROGRAM ELEMENT, PROJECT, TASK AREA & WORK UNIT NUMBERS
11. CONTROLLING OFFICE NAME AND ADDRESS Naval Research Laboratory Washington, DC 20375	12. REPORT DATE September 1982
	13. NUMBER OF PAGES 35
14. MONITORING AGENCY NAME & ADDRESS(if different from Controlling Office)	15. SECURITY CLASS. (of this report) Unclassified
	15a. DECLASSIFICATION/DOWNGRADING SCHEDULE

16. DISTRIBUTION STATEMENT (of this Report)

DISTRIBUTION STATEMENT A
Approved for public release;
Distribution Unlimited

17. DISTRIBUTION STATEMENT (of the abstract entered in Block 20, if different from Report)

18. SUPPLEMENTARY NOTES

19. KEY WORDS (Continue on reverse side if necessary and identify by block number)

silicon MBE
silicon suboxide
disilicon monoxide
disilicon trioxide
reflection electron diffraction

20. ABSTRACT (Continue on reverse side if necessary and identify by block number)

Silicon molecular beam epitaxy (MBE) was used to grow submicron undoped epitaxial Si layers on 2-inch Si substrates. The films had low defect densities. Radiative wafer heating was used, and no temperatures above 900°C were necessary. In addition, the single crystal silicon suboxides Si_2O and Si_2O_3 were grown by MBE for the first time on (111) and (100) Si substrates, with Si_2O growing primarily on the (111) wafers.

DD FORM 1 JAN 73 1473 EDITION OF 1 NOV 65 IS OBSOLETE / UNCLASSIFIED

SECURITY CLASSIFICATION OF THIS PAGE (When Data Entered)

Undoped Si films were characterized for defects with a Wright etch, and for doping and thickness with spreading resistance. The single crystal suboxides were identified by interpreting reflection electron diffraction (RED) patterns and by comparing Auger spectra with published data for amorphous SIPOS (semi-insulating polysilicon) films containing the same compounds. Capacitance-voltage results show MOS-type behavior, although with charge injection and some conductivity of the suboxide.

The Si_2O crystalline structure on (111) Si may be thought of as oxygen planes between double (111) planes of Si, with a 180° Si-O-Si bond. Crystalline Si_2O_3 is an assembly in a Si-like lattice of Si_4O_6 molecules, each of which has one tetrahedral bond per silicon atom. All other Si bonds are satisfied by 109.5° Si-O-Si bonds.

I. INTRODUCTION

This is a report on a research program in molecular beam epitaxy (MBE) at Varian, aimed at growth of silicon and silicon dioxide on silicon wafers for integrated circuits.

Three important features of MBE that affect the growth of silicon and MOS insulators were mentioned when this work was proposed. One was the ability of MBE to form atomically smooth surfaces and interfaces, and thus reduce the interface roughness component of electron scattering in MOS devices. Another was the low growth temperature of MBE, enabling the growth of thin epitaxial layers with abrupt interfaces (e.g., for bipolar integrated circuits) and possibly a stress-free oxide for MOS. Finally, the possibility of a single crystal oxide on (100) silicon (β-cristobalite, nearly lattice matched when rotated 45°) was discussed, as it would allow an interface free of dangling bonds, fixed charge, band tailing, etc.

Figure 1 is an edge-on photograph of a model of the (100)Si/β-cristobalite structure in which the observer is looking down the 010 direction in the silicon (lower) lattice, and down the $(\bar{1}10)$ direction in the β-cristobalite (upper) lattice. The perspective view in Fig. 2 better illustrates the role of the interfacial silicon and oxygen atoms. Interfacial O is bonded at a tetrahedral angle and is bonded singly, meaning that atomic O may be preferred to O_2. Also, some distortion in the interfacial Si bonds must occur to accommodate the 45° twist (that is why 26-hedrons had to be used for interfacial Si in the model).

During the course of this contract, we were able to grow undoped single crystal silicon films 3000 Å thick on 2-inch silicon wafers, having low defect densities. This growth followed heat cleaning at 850-900°C of a chemically-induced protective oxide coating. Another important result of this work was to achieve, for the first time, single

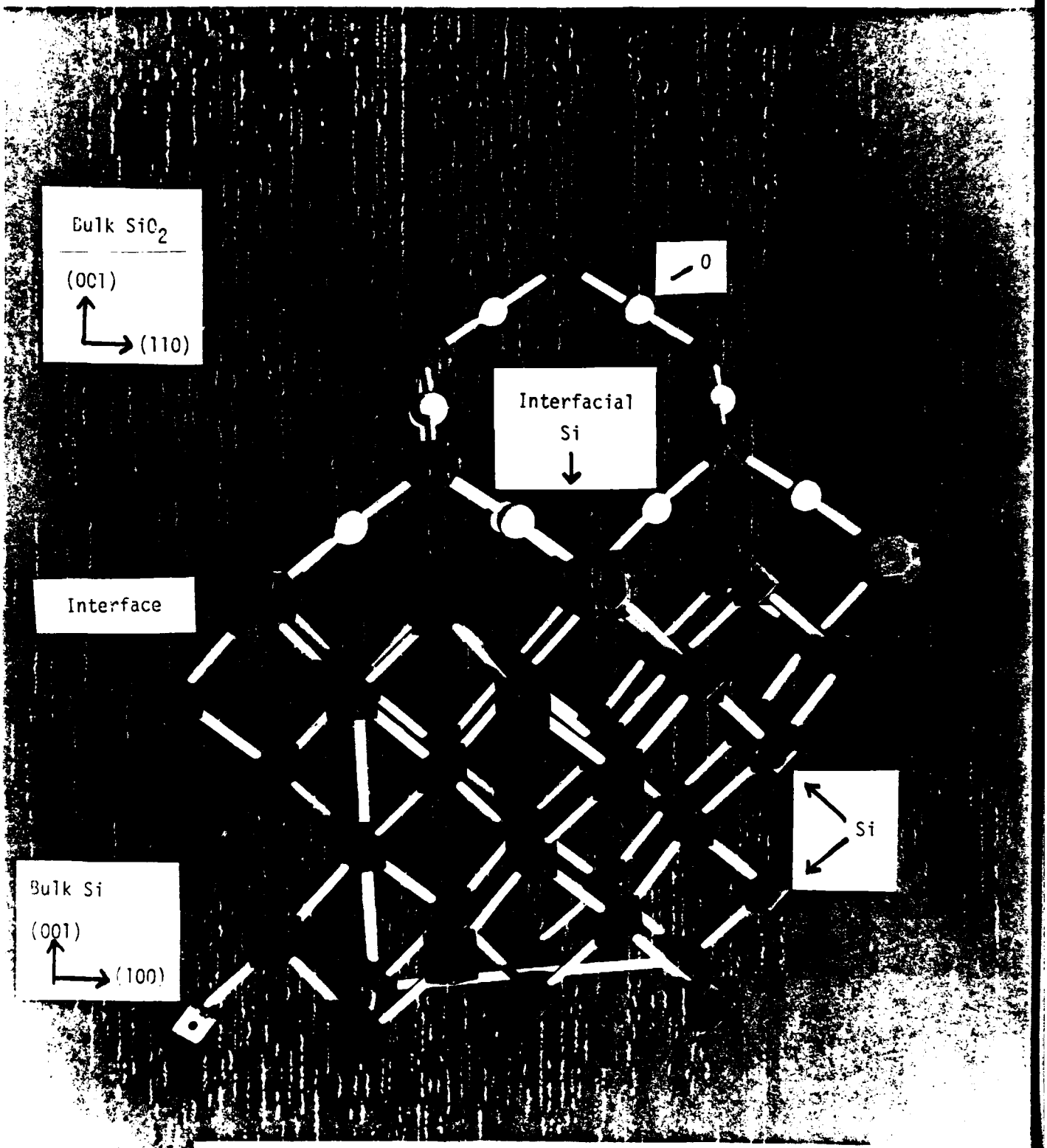

Fig. 1 Edge-on view of β-cristobalite SiO_2 on (100) Si.

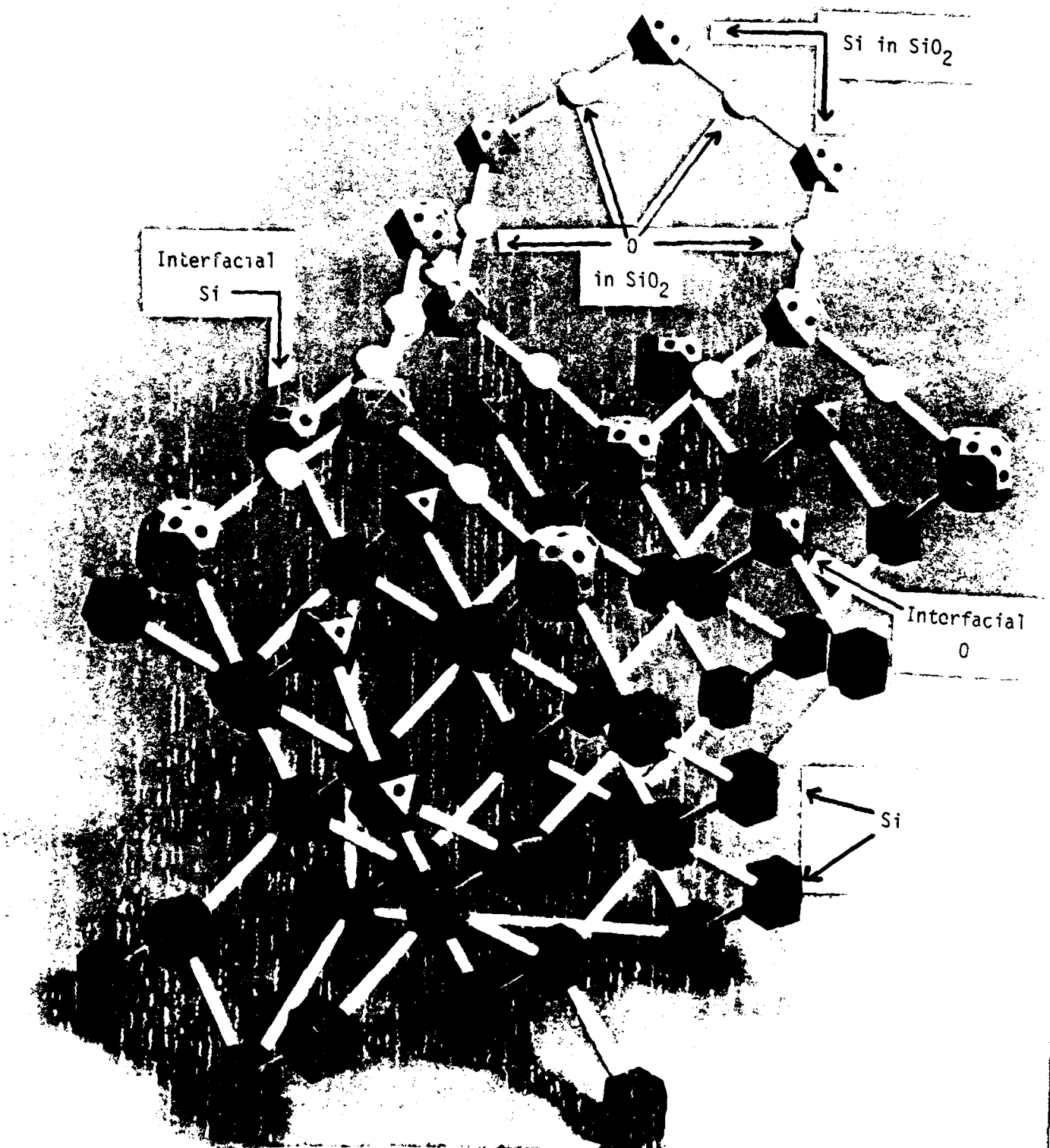

Fig. 2 -cristobalite SiO_2 on (100) Si.

crystal growth of the silicon suboxides Si_2O and Si_2O_3 on (100) and (111) substrates, at about 675°C, a serendipitous result that may have far-reaching technological consequences. Because these suboxides rapidly desorb above the growth temperature (and grow amorphously below it), that temperature can probably now be considered a lower bound for β-cristobalite growth on (100) silicon.

In the remainder of this report, there is a discussion of silicon wafer heating, a description of the MBE apparatus and procedure, and a presentation of experimental results. A discussion that follows will interpret the results in terms of the aforementioned single crystal suboxides.

II. SILICON WAFER HEATING

The Varian Gen II MBE machine was designed for epitaxy of III-V semiconductors, and the wafer heating hardware consists of a molybdenum heater block (radiated by tungsten filaments) onto which odd-size or up to 2-inch circular substrates may be attached. The usual way of heating a III-V semiconductor is to bond it to the heater block with indium. The conductive thermal contact allows the wafer to reach a temperature near that of the block itself, with the result that temperature sensing and control by means of a thermocouple in contact with the back of the heater block is feasible.

Silicon wafers are, of course, generally not odd-sized, and there is no convenient analog to indium that would not alter the wafer's electrical properties or be usable at the kind of maximum temperatures (at least 900°C) that we require for Si MBE. Thus radiative heating is very desirable, other reasons being that the heater block could eventually be left out of the vacuum cycle, and the whole process could be automated if the wafers are not disturbed. We therefore undertook a study of radiative heating of Si wafers using a slightly modified Gen-II heater block. We achieved the required high (1200-1400°C) block temperatures by floating the heater filaments as high as -600V so that most of the power (360 out of 540 W at maximum heat) comes from electron bombardment. The wafer heating study was done mostly in the early stages of this work, and was undertaken on internal funds, although it was essential to the completion of this contract.

An auxiliary vacuum system, complete with MBE load lock, transfer equipment and CAR (continuous azimuthal rotation unit, which contains the wafer heating station), was used since at the time the Gen II was still being installed and initiated.

Initial efforts to use emission current to heat the heater block were plagued by instabilities in the temperature control loop (which includes a Eurotherm PID controller) because, in the simplest configuration, the controller regulates only the filament voltage and current. But since beyond a certain point the emission current is very sensitive to filament current, it was easy to throw the control loop into oscillation whenever the filament floated at a substantial negative voltage. This problem was solved by taking careful I-V data for both filament and emission current and voltage, and by sensitizing (with a 10-turn pot) the filament current limit, which must be carefully set on the filament power supply. Emission voltage can then be fine-tuned to stabilize the temperature control system. One can imagine additional electronics to regulate emission voltage as well as the filament (emission voltage alone is not sufficient), but this design effort was not undertaken. Some adjustment of filament conditions must be made when oxygen is introduced into the vacuum chamber, since oxygen raises the work function of tungsten and thus reduces the emission current for a given filament bias.

The wafer is held onto the heater block with W/26% Re clips which, because of the rhenium content, will not become brittle after intense heating. A 0.005" recess machined into the block separates all but the very edge of the wafer from the heater block and allows true radiative heating. The small amount of conductive heating from the rim often balances out the radial temperature drop that would otherwise occur. At the block temperatures used, the Si wafer reacts with the Mo block to form Mo silicides, and resulting hot spots, so the wafer is isolated from the Mo in the heater block by one of three techniques. The method used in all of the wafer growths reported here was to coat the block with SiO_2 by chemical vapor deposition (CVD). Coating the back of each wafer also works, but is incompatible with our chemical wafer preparation method (next section). Another was to sputter coat the block with

SiC and then vacuum fire it, giving a dark, highly emissive coating. This method suffered from slow desorption of the coating and may have been caused by oxygen in the SiC, which was noticed on an Auger scan. The sputtering machine is located within Varian and there is hope for future progress. However, the SiC coating lasted long enough to measure the improvement in wafer heating efficiency that resulted from its higher emissivity. The third method of separating the wafer from the heater block was to mount a 2" quartz disk between the wafer and the block, which served as an infrared window for the radiation.

Figure 3 gives the relation between the wafer temperature (measured with an optical pyrometer) and the block temperature (W-5% Re/W-26% Re thermocouple measurement; millivolt reading and °C are given) for the three alternatives. An emissivity ε of 0.7 was used for the Si wafer in the pyrometer measurements.[2] This did not account for the unknown losses in the pyrex vacuum window, which may explain why when the Si-Al eutectic transition (577.2°C) was observed with the pyrometer, $\varepsilon = 0.58$ was measured, and why the ε of the Mo block (0.1) and the SiC coated block (0.5) were lower than expected, ignoring gradients in the block itself. Thus the wafer temperatures quoted may actually be higher (about 45°C at the top end) than indicated.

The quartz disk method seemed to give the most uniform heating of the wafer and looks very promising for the future except that at present a very hot block is required to achieve the wafer heat-cleaning temperature (850-900°C). There is also a problem with thermal slip lines (often near the wafer clips) in all methods, except that the quartz disk method is remarkably free of them until above 800°C. Improvement of heating efficiency for this method (perhaps with SiC coating of the block) is thus desirable. SiC coating of the back of a quartz disk is another possibility.

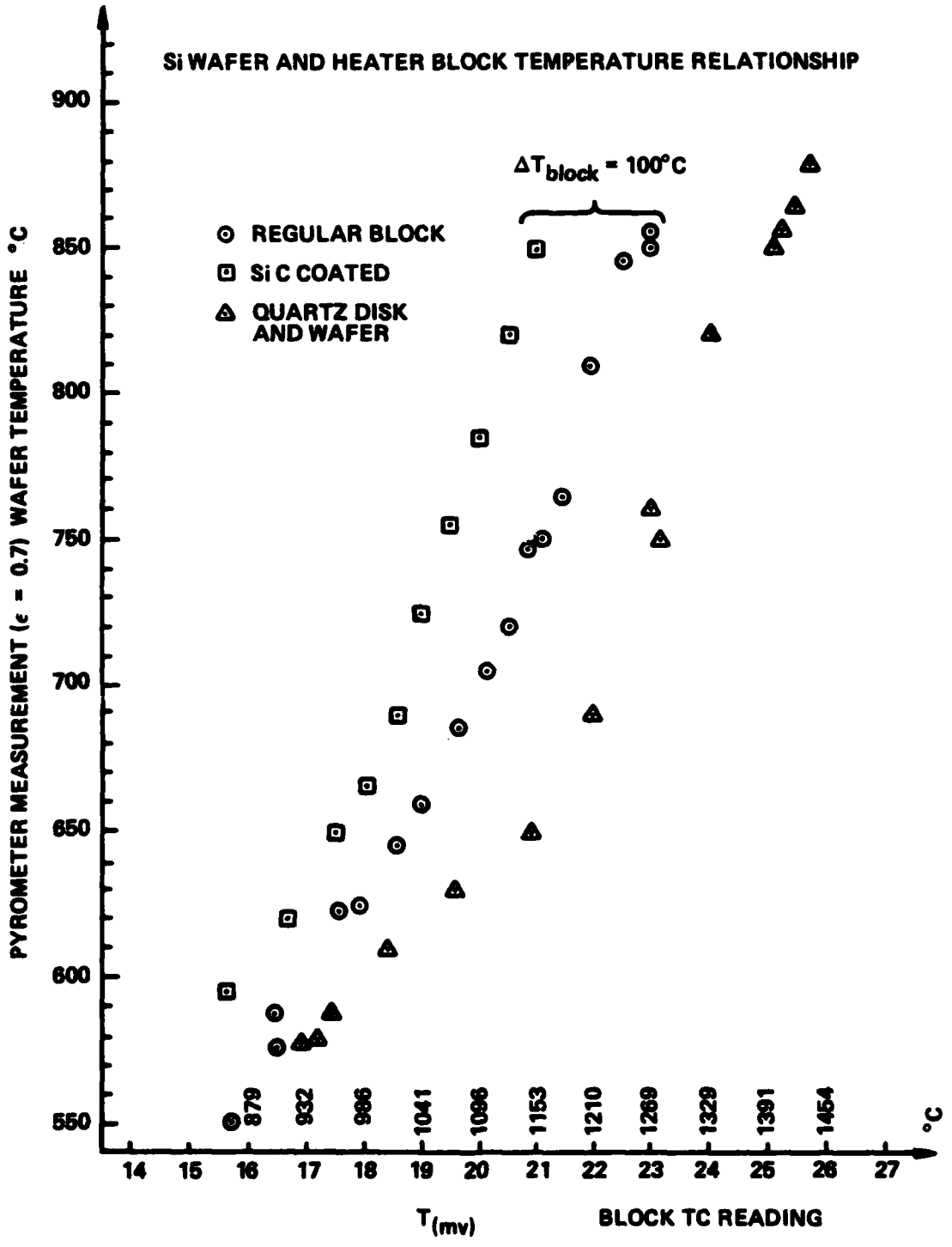

Fig. 3 Silicon wafer and heater block temperature correlation.

III. EXPERIMENTAL APPARATUS AND PROCEDURE

The Varian Gen II MBE machine as configured for silicon epitaxy is shown in Fig. 4. The major differences to note are the absence of a source flange with the usual III-V sources, and the two e-beam evaporator sources which are used for silicon.

The preparation/analysis (or prep) chamber and growth chamber are always under high vacuum, and a separately pumped load lock helps to transfer wafers in and out. Auger analytical instruments (and an associated sputter gun) are available in the prep chamber. There are six wafer stations, including two heater stations, on a carousel in the prep chamber. The growth chamber has more analytical equipment: A quadrupole mass spectrometer (QMS) and a reflection electron diffraction (RED) gun. High vacuum pumping in the Gen-II is generally achieved by ion pumps; the growth chamber is pumped by a 400 l/sec ion pump as well as a Ti-ball pump and a liquid nitrogen-cooled cryoshroud that surrounds the CAR and wafer.

Two-inch silicon wafers are first chemically cleaned[3] in quartz beakers so as to leave a thin protective oxide coating on the surface. Just prior to loading the wafers into the Gen II load lock, the wafer is mounted with W/26% Re clips onto a Mo heater block, which is transferred along with the wafer into the Gen II prep chamber. Several hours of outgassing at 720°C (block temperature; wafer temperature is 400-450°C and the protective oxide is not affected) follow, before transfer to the growth chamber. Immediately before epitaxial growth in the growth chamber, the protective oxide is heat cleaned away at 850-900°C, as the wafer is radiatively heated by a Mo heater block at about 1270°C. An Auger study of this heat cleaning showed less carbon contamination than Henderson,[3] and no boron contamination at all, due to the use of quartz beakers rather than Pyrex. Although higher wafer temperatures (1100-

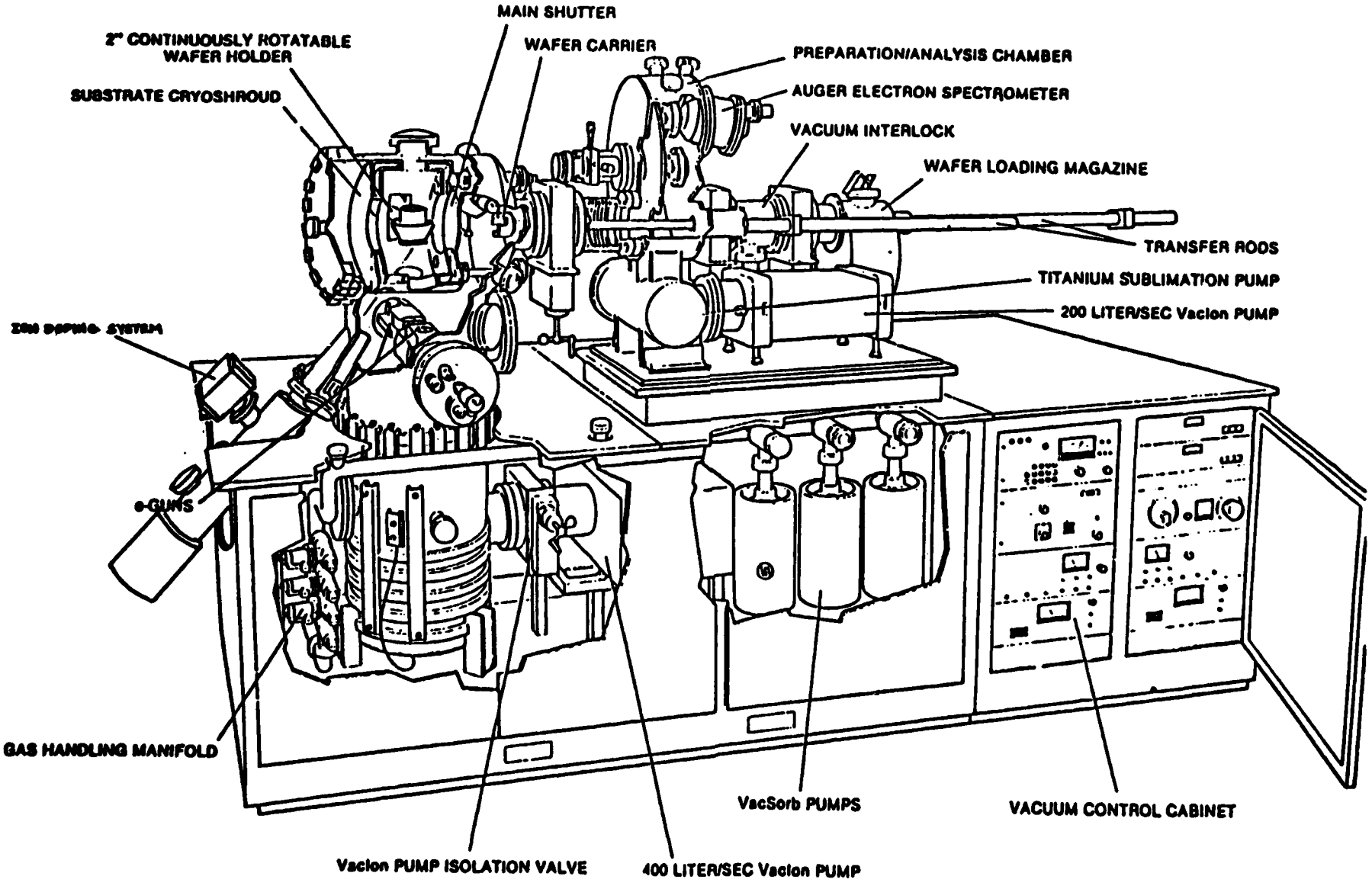

Fig. 4. Varian Gen II MBE machine, adapted to Si epitaxy.

1200°C) are often used to desorb surface carbon, these heat cleaning temperatures have been used successfully by others to grow defect-free films.[4]

Silicon is evaporated from one of two 45 cm^3 sources, each in an Airco Temescal e-beam hearth some 35 cm from the wafer. The source-to-wafer direction is about 30° with respect to the vertical, which tends to minimize epitaxial defects due to spitting from the melt. Azimuthal rotation of the wafer greatly improves the uniformity of the epitaxial film.

For the MBE oxide experiments, silicon was evaporated in the presence of O_2, which was leaked into the chamber to a pressure of 3-5 x 10^{-6} Torr by a variable leak valve attached to a T-purged gas system fed by a tank of research grade O_2 (Fig. 5). During these runs, the Si melt was seen to function as an oxygen getter pump; i.e., when the Si melt was shuttered, O_2 pressure would rise sharply, say from 2.5 x 10^{-6} Torr to 5 x 10^{-6} Torr. This was because there was no longer any silicon being deposited on the walls of the system and reacting with any available oxygen. The amount of O_2 pumping by Si was seen to be a sensitive measure of the silicon flux, as confirmed by the beam flux gauge (an ion gauge mounted on the CAR and rotated into the precise location of the wafer) and the QMS. The effect was easily employed in a later experiment in which the melt was repeatedly shuttered in an effort to increase oxygen content in the film (see next section).

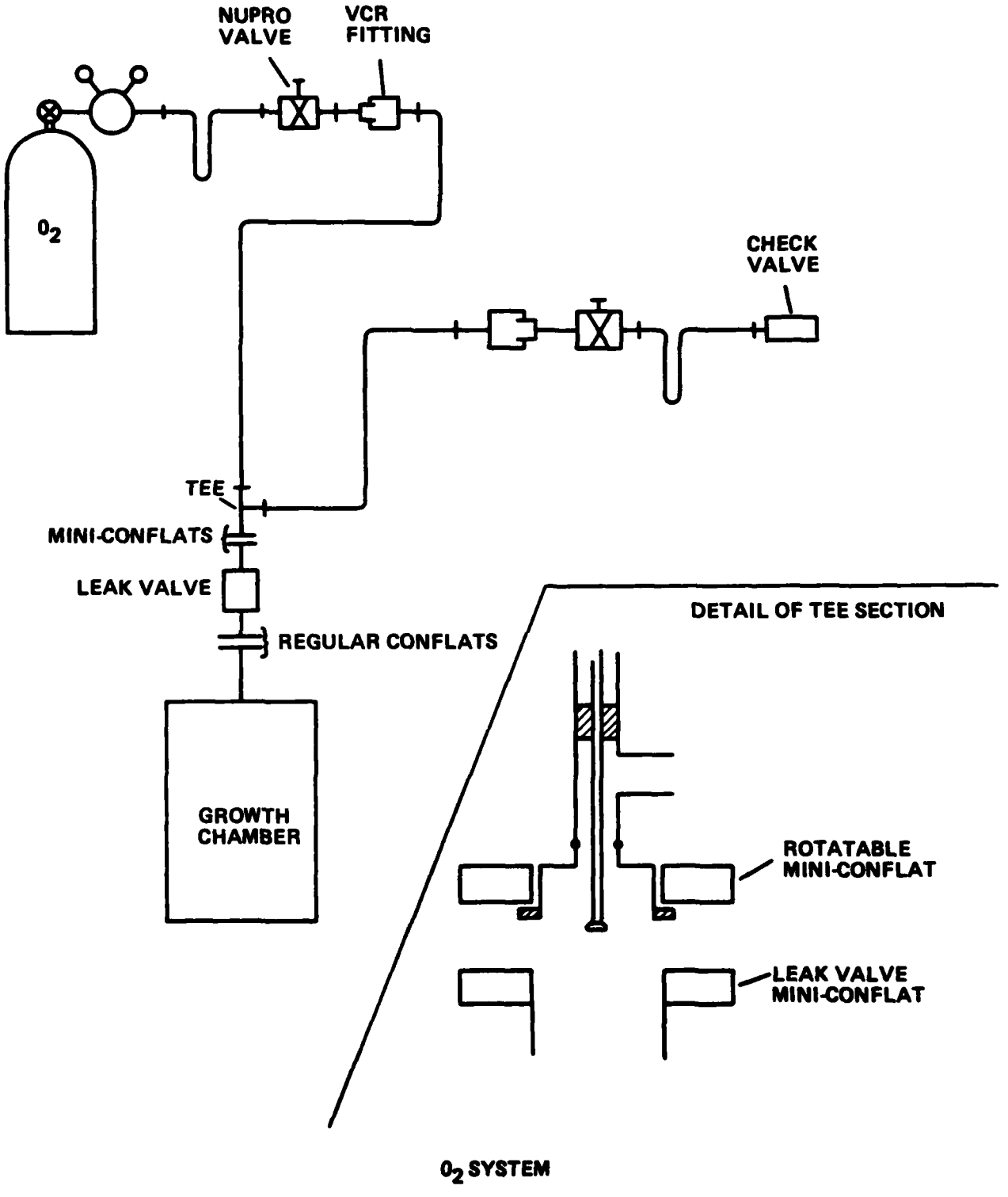

Fig. 5 Oxygen gas inlet system with purged tee.

IV. SILICON AND OXIDE FILM GROWTHS

A. Undoped Silicon Epitaxy

Once the MBE machine was ready for use, undoped layers of silicon were immediately grown on a p(100) substrate and a p(111) substrate for 1 hour apiece at 850°C. Film thicknesses of 2500-3000 Å were measured by Mirau interferometry (on a Zeiss microscope) and by spreading resistance. Some time later another (100) film was grown, this time for one-half hour at 765°C. 3000 Å film thickness was measured by Mirau interferometry for this layer, meaning that 6000 Å per hour growth rate was achieved. However, there may have been a slight buildup of silicon near the edge of the shadow mask (a scrap of Si) that was used to create a step. One other attempt to grow on a (111) wafer was made, but by that time the Si melts were depleted and the necessary beam flux could not be achieved.

Spreading resistance plots for the first two silicon epitaxial layers (SM-1 and SM-2) are shown in Figs. 6 and 7. In each case the epitaxial layer appears to be about one-fourth micron thick. The doping of each substrate to a depth of several microns is unexplained (these substrates came from different manufacturers) but may have been due to some kind of fast-diffusing impurity in the film.

Several etches were used to resolve defects in the epitaxial films, the most successful being the Wright etch.[5] The (100) layers had low defect densities, around $100/cm^2$ in clear areas of the wafer. There were a few patchy clusters of high defect densities on the (100) wafers, especially near the edges, but these could have been due to wafer handling. The lone (111) wafer had a uniformly high density of triangular defects (about $10^5/cm^2$), but this could have been because during the growth run (the second ever done on this machine) there was a momentary loss of vacuum and buildup to 10^{-5} Torr pressure in the vacuum chamber.

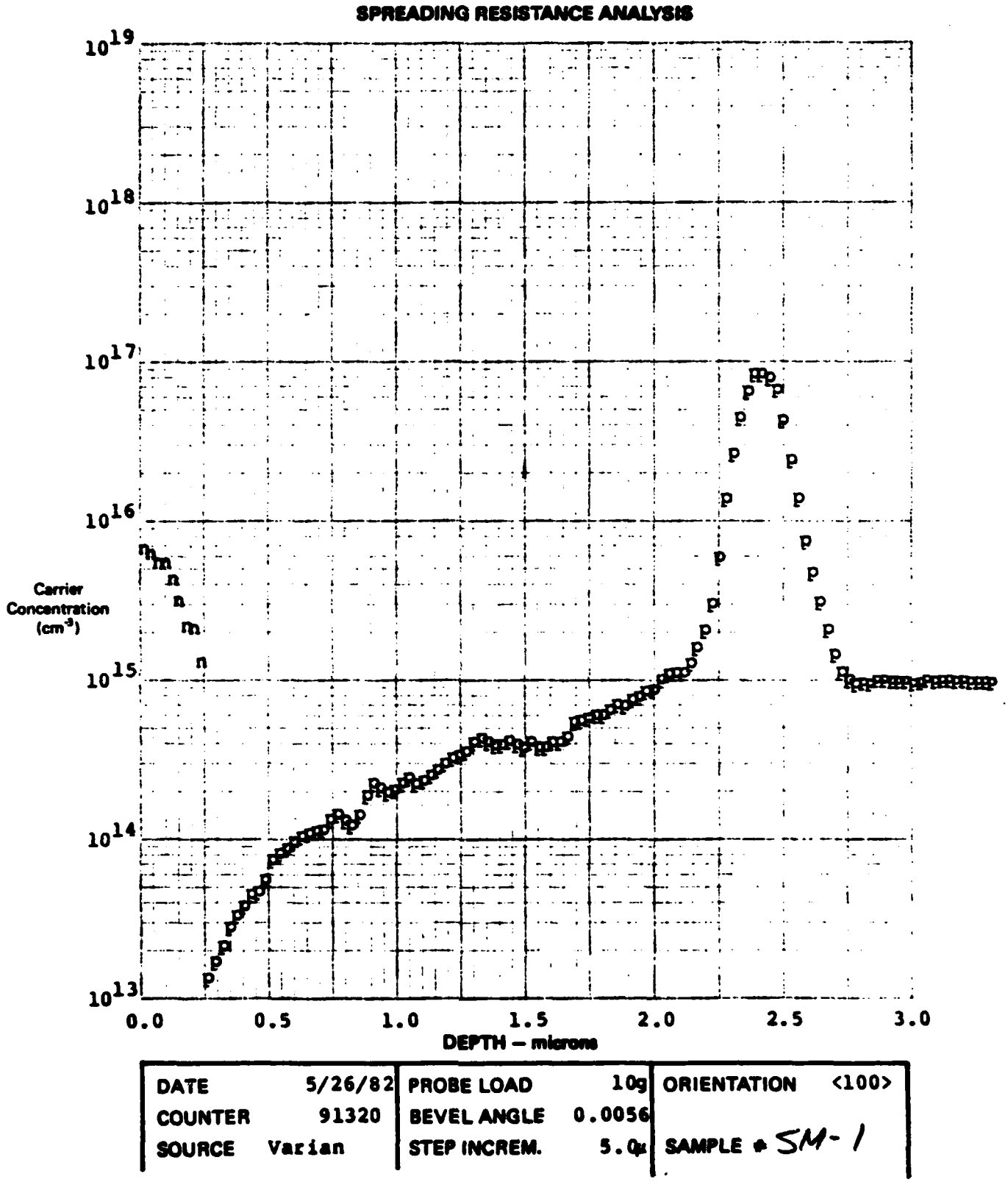

Fig. 6 SM-1 ((100) undoped Si) spreading resistance analysis.

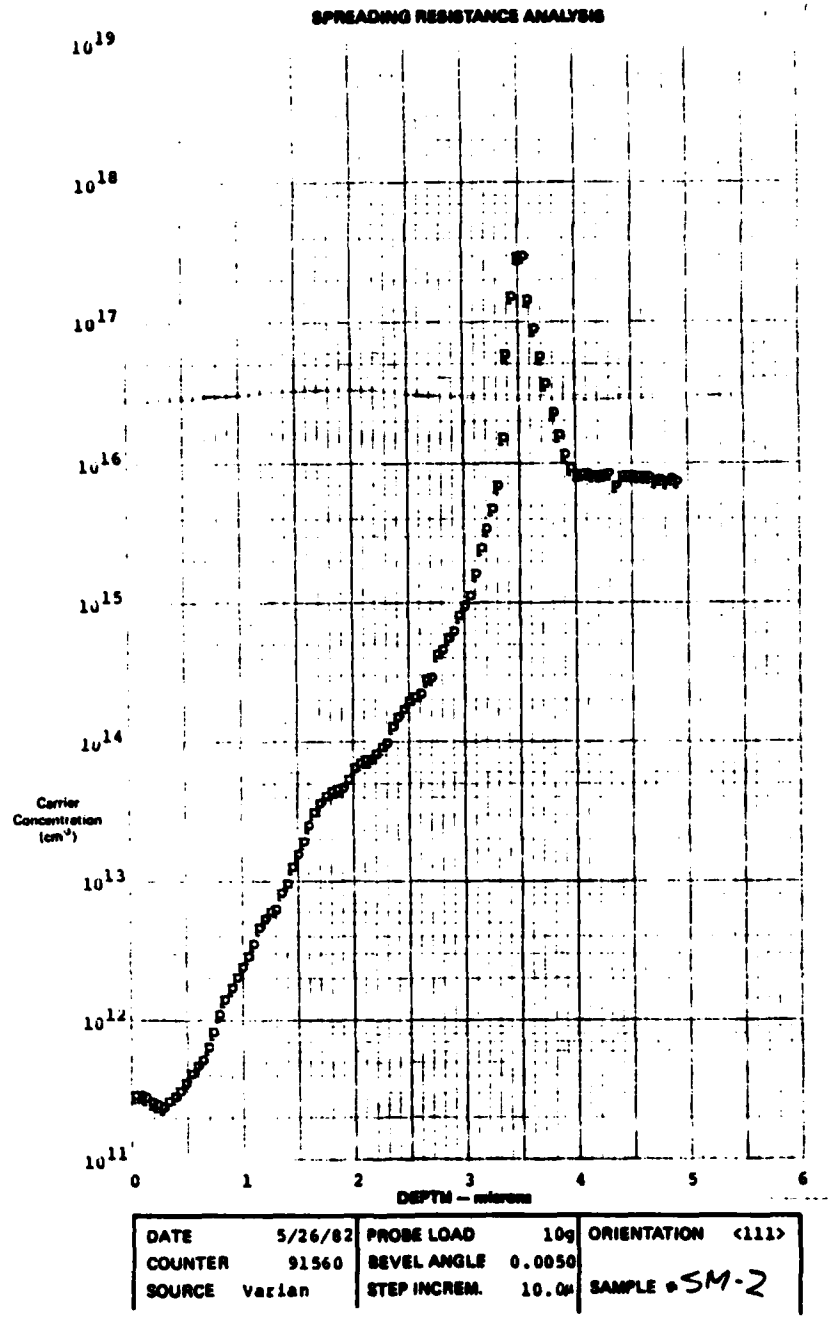

Fig. 7 SM-2 ((111) undoped Si) spreading resistance analysis.

As mentioned in Section III, heat cleaning by desorption of the chemically-induced protective oxide layer was used to prepare the surface for Si epitaxy. RED patterns for the heat cleaned surfaces are shown in Fig. 8. In the early stages of the oxidation studies, it was noticed that oxygen-containing films could be desorbed at 850°C to leave a very smooth surface, as indicated by streaks in the RED pattern (Fig. 9). For this reason, SM-6 (the other (100) Si epilayer) underwent desorption of a grown MBE oxide layer along with the initial heat cleaning proceding that oxide growth. As we will later see, the MBE oxide at present may be only about 25-35% O, meaning that some of the deposited Si may be left after the heat cleaning, but the procedure was adequate for this undoped film.

B. Oxygen-Rich Silicon: Ordered and Disordered Structures

MBE oxides were grown by evaporating Si in the presence of O_2, as described in Chapter III. Some excitation and dissociation of the O_2 can be expected from the ion gauges and the electron flux from the Si e-beam melt, which may facilitate the oxidation process. The silicon flux was from 0.1 to 0.2 times that used for the 3000 Å/hour undoped Si layers, and the O_2 pressure was between 2.5 and 5 x 10^{-6} Torr. Toward the end of this work, in an effort to increase the oxygen content of the MBE oxides, the Si melt was shuttered for half the operating cycle time (30-sec periods) so that the oxygen could saturate the surface. As mentioned earlier, the Si flux getter pumped the O_2 in the chamber. The effect was used to monitor the Si flux and to indicate when the Si surface was saturated.

Table I is a summary of data for the successful MBE oxide wafers. Temperatures are estimated from Fig. 1. All of these wafers had color fringes reminiscent of SiO_2 films and, except as noted on Table I, were mirror smooth. Ellipsometric measurement of the film thickness using an automatic ellipsometer with a 6328 Å laser was not successful, however,

(a) (100) Si
1

Fig. 8 RED patterns of heat cleaned a) (100) and b) (111) Si.

(b) (111) Si
1

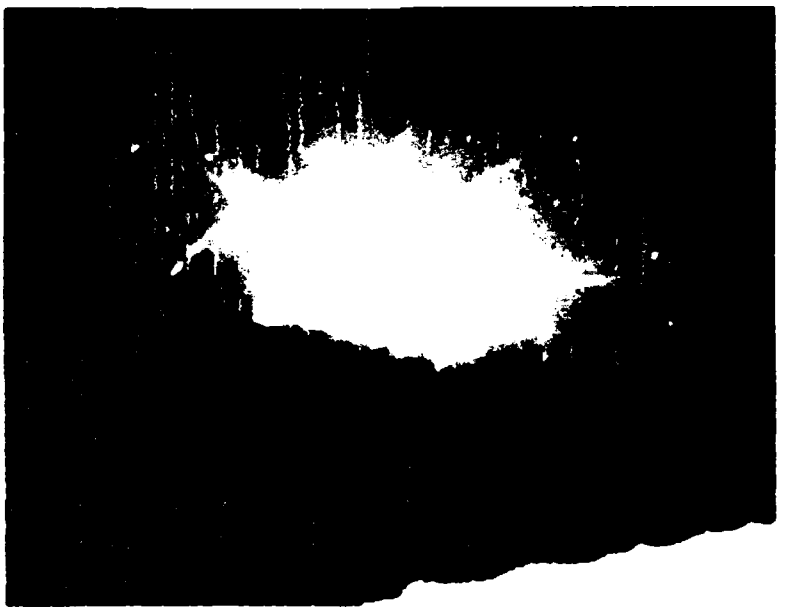

(100) Si
2

Fig. 9 RED patterns of desorbed MBE oxide.

(100) Si
3

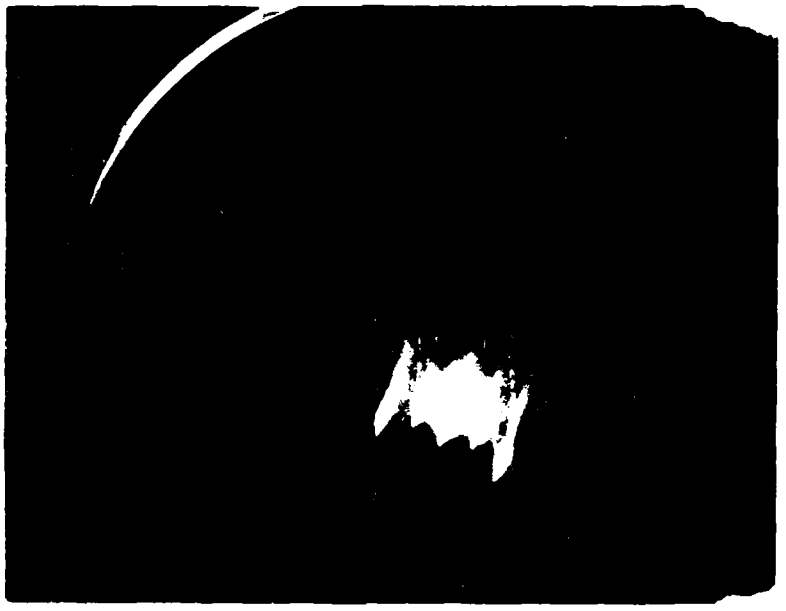

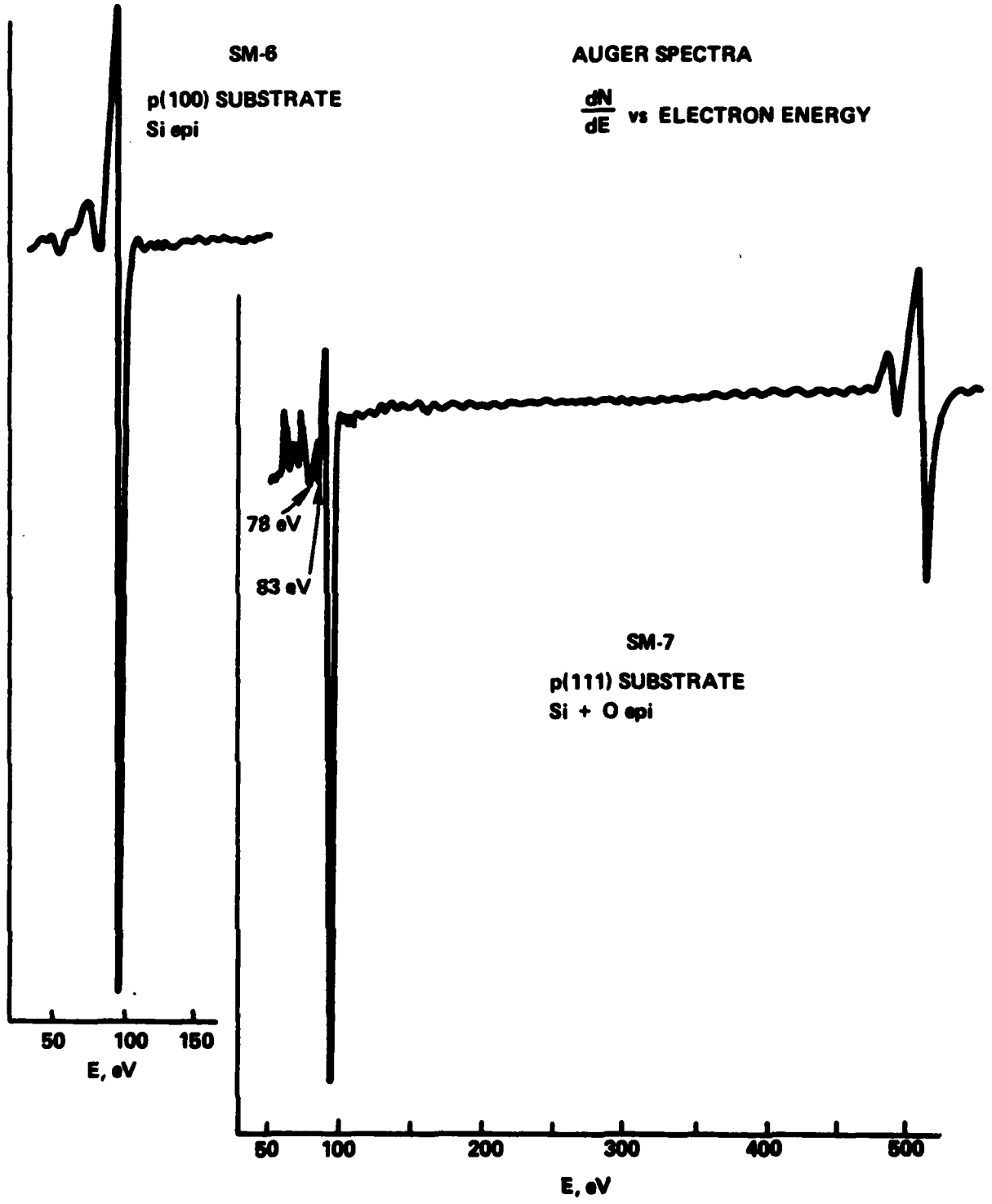

Fig. 10 Auger spectra of pure Si and oxidized Si MBE epitaxy.

TABLE I: SUCCESSFUL MBE OXIDE WAFERS

Wafer	Growth Temp. °C	% O Estimated	Single Crystal?	Growth Time	Remarks
SM-7, (111)	675	25	yes	10 min.	
SM-8, (100)	675	18	yes	10 min.	Grew 5 min. Si first
SM-9, (100)	675	25	yes	13 min.	
SM-10, (111)	670	17	yes	10 min.	Slightly fogged; heat cleaned and regrown five times.
SM-11, (111)	670	24	yes	10 min.	
SM-13, (100)	675	26	yes	15 min.	
SM-14, (100)	640	38	no	90 min.	Surface fogged, low Si flux.
	Growth Chamber Opened, Si Melts refreshed, Chamber Baked Out				
SM-17, (100)	640	24	no	100 min.	Si shuttered 30 sec. of each minute.
SM-18, (100)	200	30	no	100 min.	Same as SM-17

possibly because of attenuation. A photoluminescence measurement (Ar 5145 Å line) was done on SM-7 and SM-9, but the result was the same as that obtained with a plain Si wafer. This is not too surprising because the film thicknesses for all the 10-15 minute runs were about 500-600 Å (stylus measurement). Mirau interferometry on the 90-minute run, SM-14, gave 1000 Å. A reliable photoluminescence experiment will have to wait for much thicker oxygen-doped layers.

Oxygen percentages were estimated for Table I from Auger data and known sensitivities for Si and O at 5 kV. Typical Auger spectra for the oxides (Fig. 10b) contained a pronounced silicon peak that was more like the peak for pure silicon (Fig. 10a) than the silicon peak for SiO_2 (Fig. 11), which is broadened and chemically shifted to lower energy. However, the shape of the 92 eV free Si peak for the MBE oxides is not quite like that of pure Si, and also there seem to be some chemically-induced extra lines at 78 and 83 eV. This is precisely what was observed when Auger spectroscopy was done on SIPOS layers[6] containing the amorphous suboxides Si_2O and Si_2O_3. The next section will discuss this further. Oxygen percentages may have been too low because of desorption by the electron beam.

Four wafers (SM-7, SM-9, SM-11 and SM-13), two of each orientation, were chosen for capacitance-voltage characterization. At first, samples were prepared as thermally oxidized wafers would be: Aluminum dots 0.020" in diameter were evaporated onto the sample using a shadow mask, then the wafer was annealed in H_2 at 450°C for 30 minutes. The result was usually very poor C-V characteristics and high leakage between dots and between a dot and the substrate. Only a very few dots were as in Fig. 12, which includes a plot of conductance G (in micromhos) as well. It was felt that the free silicon in the MBE layer had probably alloyed with the Al dot metal, causing a direct ohmic connection to the substrate. I-V characteristics seemed to bear this out.

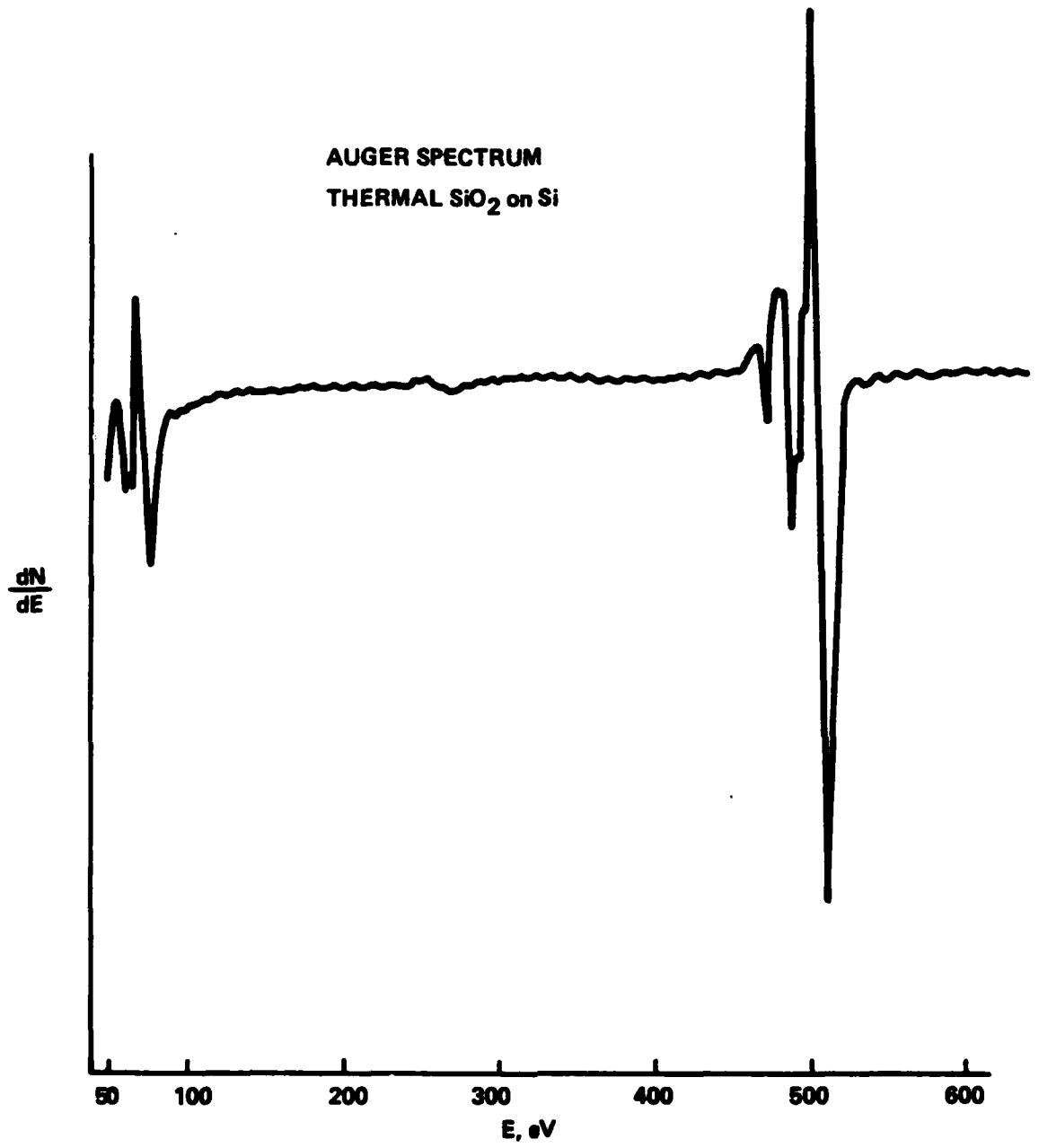

Fig. 11 Auger spectrum of thermally grown SiO_2.

Fig. 12 C-V and G-V of SM-11 at 1 MHz.

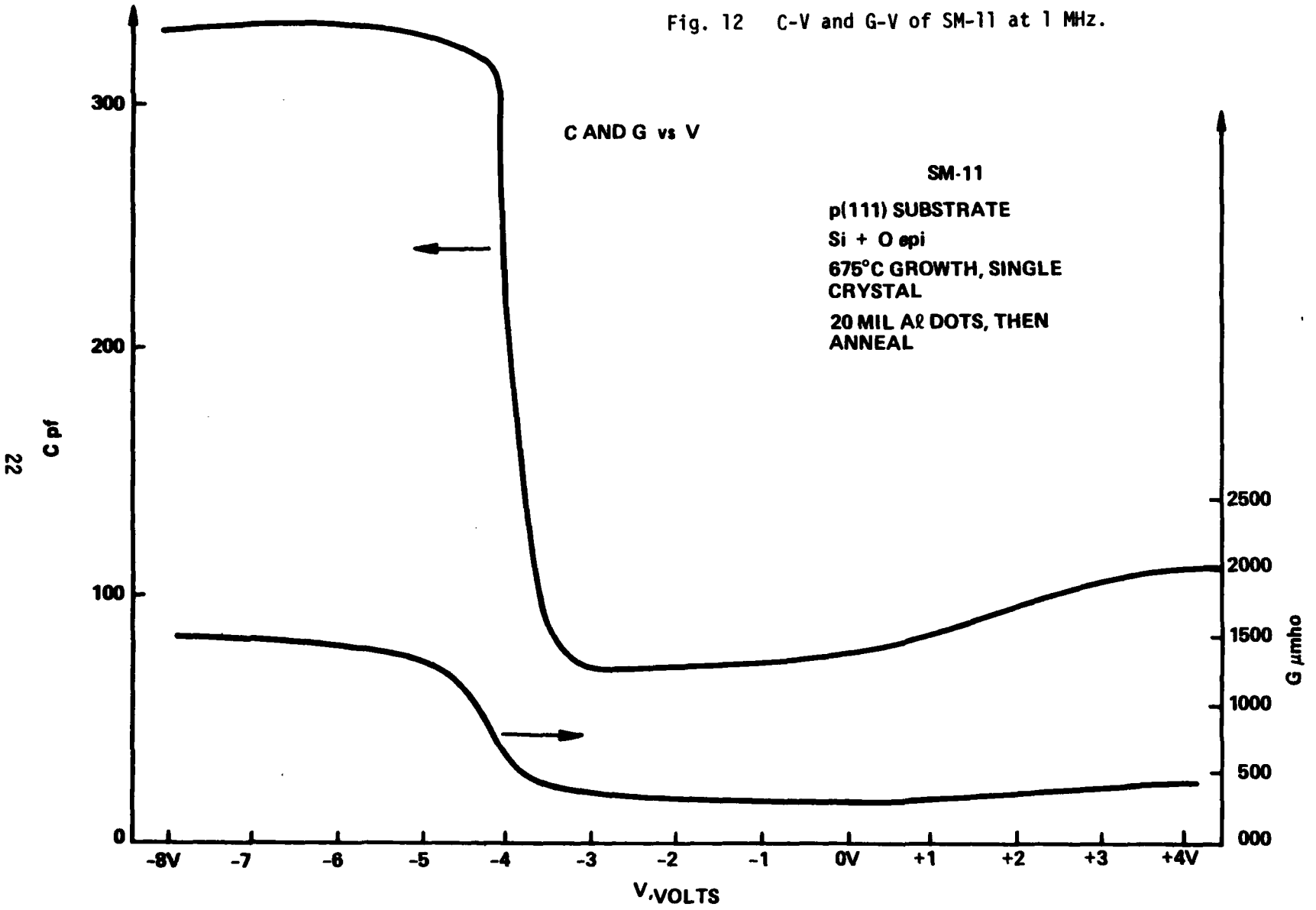

Things were vastly improved by using the Al dots without an anneal, as indicated by Fig. 13. Not only was the yield of usable dots much higher but leakage was dramatically reduced, as indicated by I-V measurements and by the conductance scale in Fig. 13. For the "100-monolayer" sample SM-18 (Fig. 14), the best result arose from annealing at 450°C in H_2 first, then evaporating the Al dots.

Figure 14 is an example of accumulation on n-type material, which occurred because a thin undoped layer was grown before the MBE oxide. The hump in the conductance probably occurs because at that point the epi-to-substrate diode (with large area and a lot of reverse leakage) is becoming forward biased while the MBE layer is not fully depleted. Notice that when the latter is depleted (and the semiconductor inverted), the conductance is very low (also evident in Figs. 12 and 13), a feature that could be beneficial for MOSFET applications.

The oxide parameters can be deduced from the C-V data if either the dielectric constant or the film thickness is known. From a [illegible] measurement, 500-600 Å was estimated as the thickness for the 10-15 minute runs. The 330 pf capacitance in Fig. 12 then gives a relative dielectric constant $\varepsilon = 9.2$, but that capacitance may be too large because the silicon and aluminum may have alloyed down to very near the substrate. The unannealed aluminum dots give lower capacitance (Figs. 13 and 14) and point to an ε between 1.5 and 3 ($\varepsilon = 1.67$ in the case of Fig. 11). Values of C_{min}/C_{max} were used to estimate the doping of the accumulated semiconductor layer, usually in the low $10^{15}/cm^3$ ((100) wafers) to high $10^{15}/cm^3$ ((111) wafers) range, characteristic of the substrates (Figs. 12 and 13). Sometimes lower or n-type dopings were observed (Fig. 14), where it was the undoped silicon epitaxy underneath the layer that was being accumulated.

Fig. 13 C-V and G-V of SM-9 at 1 MHz.

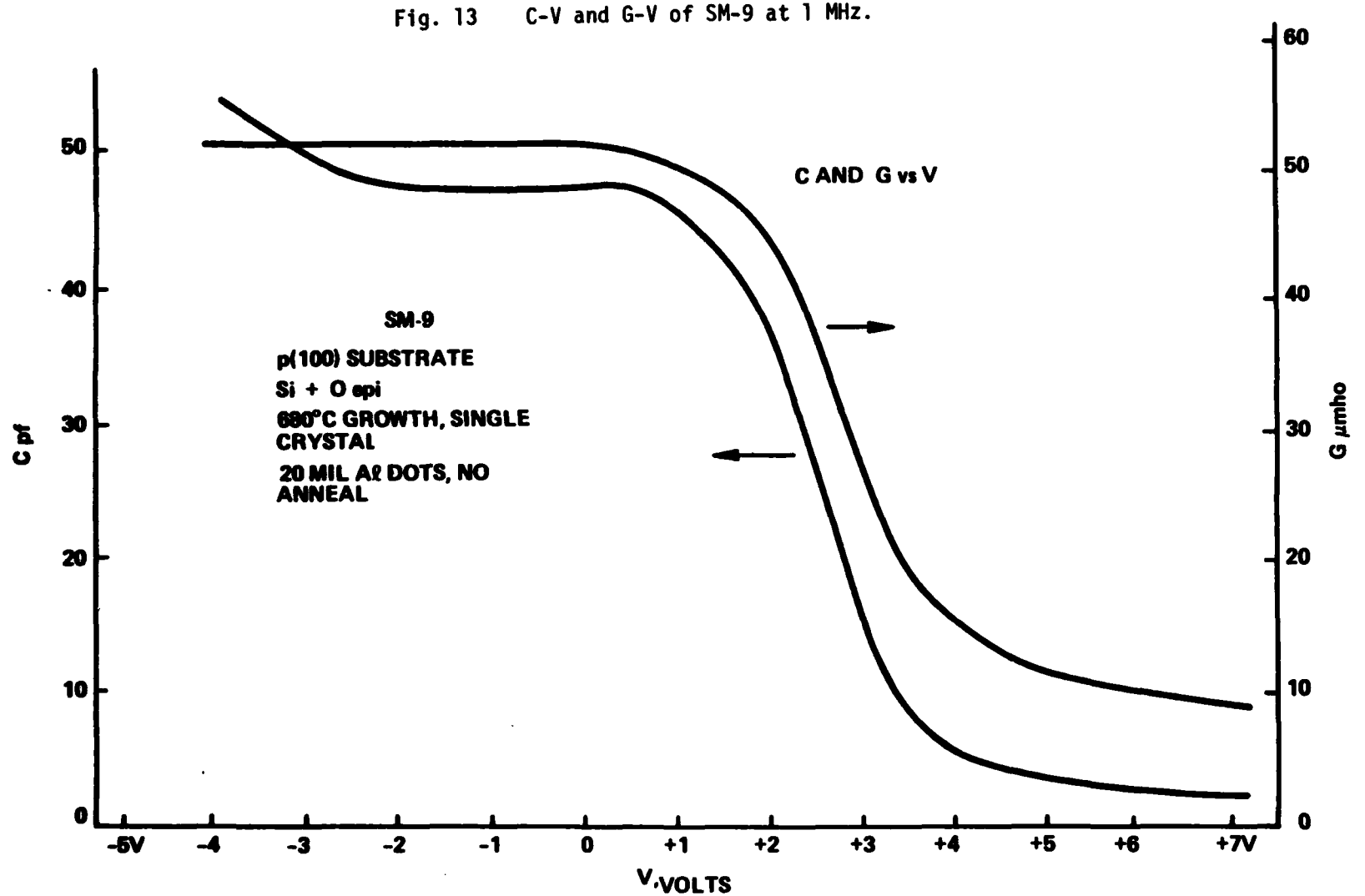

Fig. 14 C-V and G-V of SM-18 at 1 MHz.

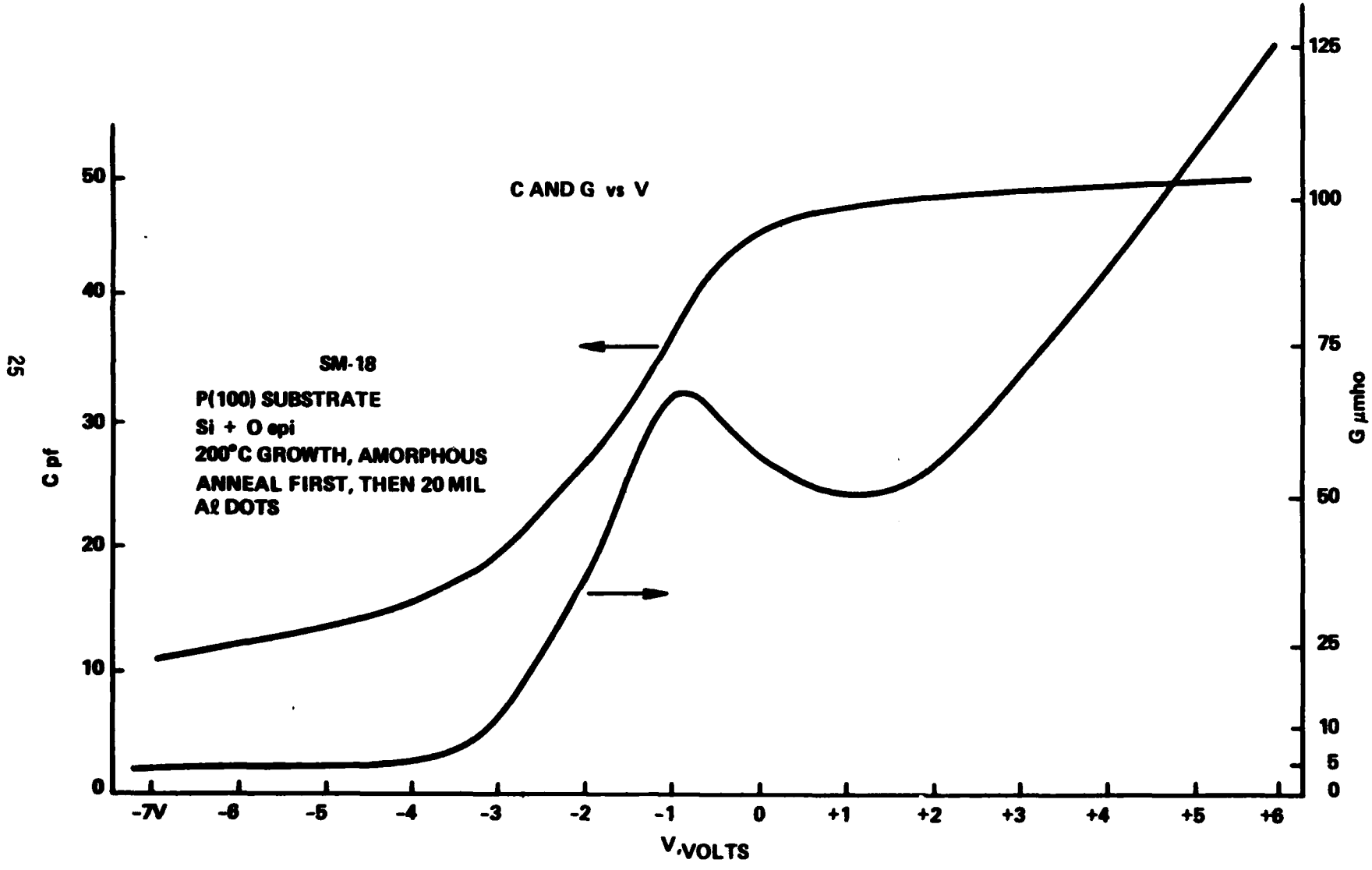

C. Discussion

The preceeding section has outlined an intriguing set of experimental results for our MBE oxide. The material is silicon rich, is single crystal, and it conducts and depletes, but must have a higher bandgap than silicon (1.11 eV) because of its C-V characteristics. The color fringes also point to a high bandgap, but the failure of the ellipsometer (1.96 eV line) to measure film thickness points to a bandgap below 2 eV. If a layer 0.5-1 micron thick can be grown, photoluminescence may reveal the bandgap. With the existing layers and metallizations, a photoconductivity experiment using a monochromator could determine the bandgap.

As we mentioned in the Introduction, one would expect some difficulty in growing β-cristobalite SiO_2 rotated 45° on (100) Si because of the distorted interfacial silicon bonds and because the lattice constant of β-cristobalite (a_o = 7.16 Å) is about 7% short of $\sqrt{2}$ times the Si lattice constant (a_o = 5.43 Å). We were clearly not able to grow β-cristobalite on Si (100), but we have a hypothesis for what happened in the (111) as well as the (100) cases, and it is related to the fact that Auger data indicate Si_2O and Si_2O_3 suboxides.

Imagine a (111) silicon surface which interfaces to a structure exactly like (111) silicon except that the vertical Si-Si bonds alone (in the (111) direction) are interrupted by oxygen with (as in β-cristobalite) 180° bond angles. A lattice model is shown in Fig. 15, with the bottom two layers being pure Si. Another way of describing this structure is to say that a plane of oxygen lies between double planes of (111) silicon atoms. The chemical formula for the epitaxial structure is Si_2O, since each oxygen atom is shared by a silicon above and below it.

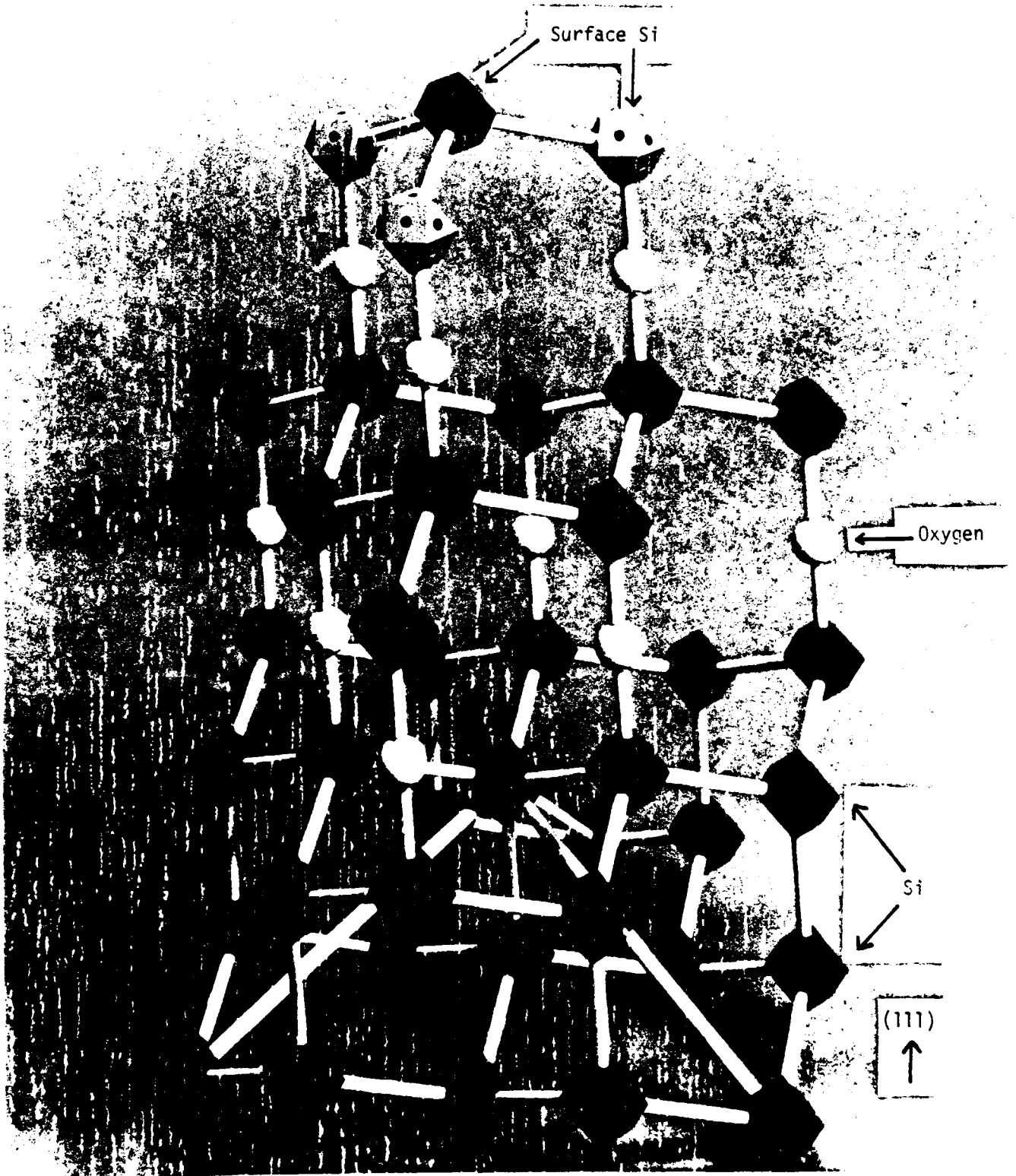

Fig. 15 Si_2O lattice model, matched to (111) Si.

Now imagine a Si_2O_3 structure in the form of a four silicon, six oxygen "superatom" with tetrahedral bonds as shown in Fig. 16. Here the oxygen bond angle is 109.5°. From the tetrahedral symmetry and structure of this molecule, it is clear that the Si-O-Si bond length determines the size of the tetrahedron, and that the structure will lattice match to Si when the new lattice constant becomes 3 times the Si lattice constant. One could expect Si_2O_3 to grow on either (100) or (111) Si. On (111) Si, one may find the hybrid $(Si_2O_3)_2O$, since Si_2O_3 behaves as a Si atom.

Si_2O is perfectly lattice matched to (111) Si and satisfies all Si bonds tetrahedrally. Its growth could proceed from ordinary oxygen attachment to the (111) surface, i.e., the bridging of dangling vertical Si bonds by O_2 molecules. When more Si falls onto the surface, the oxygen becomes "verticalized" and a new monolayer of Si is formed which can itself be O_2 bridged. Even if the Si-Si lateral bonds have been attacked at the surface by O,[7] verticalization of O bonds when new Si arrives is encouraged by the resulting lattice match.

Our Auger data at 5 kV indicated that O content in most of the films was about 25%, not the 33-60% that one would expect from the Si_2O and Si_2O_3 suboxides. But as mentioned before, there was excellent agreement with the Auger studies of SIPOS Si_2O and Si_2O_3 in amorphous form,[6] and much oxygen could have been desorbed by the Auger electron beam. Free Si would seem to have difficulty fitting into either the Si_2O or Si_2O_3 lattice structure, although it would explain leakage, depletion and failure of ellipsometry. A serious investigation should be done with ESCA before conclusions are drawn. In any case, it will be important in the future to discern the effect of the presence or absence of excited or atomic oxygen upon growth. An oxygen exciter, using a tungsten filament floating at a negative potential near the inlet port for oxygen, has been constructed and is now being tested.

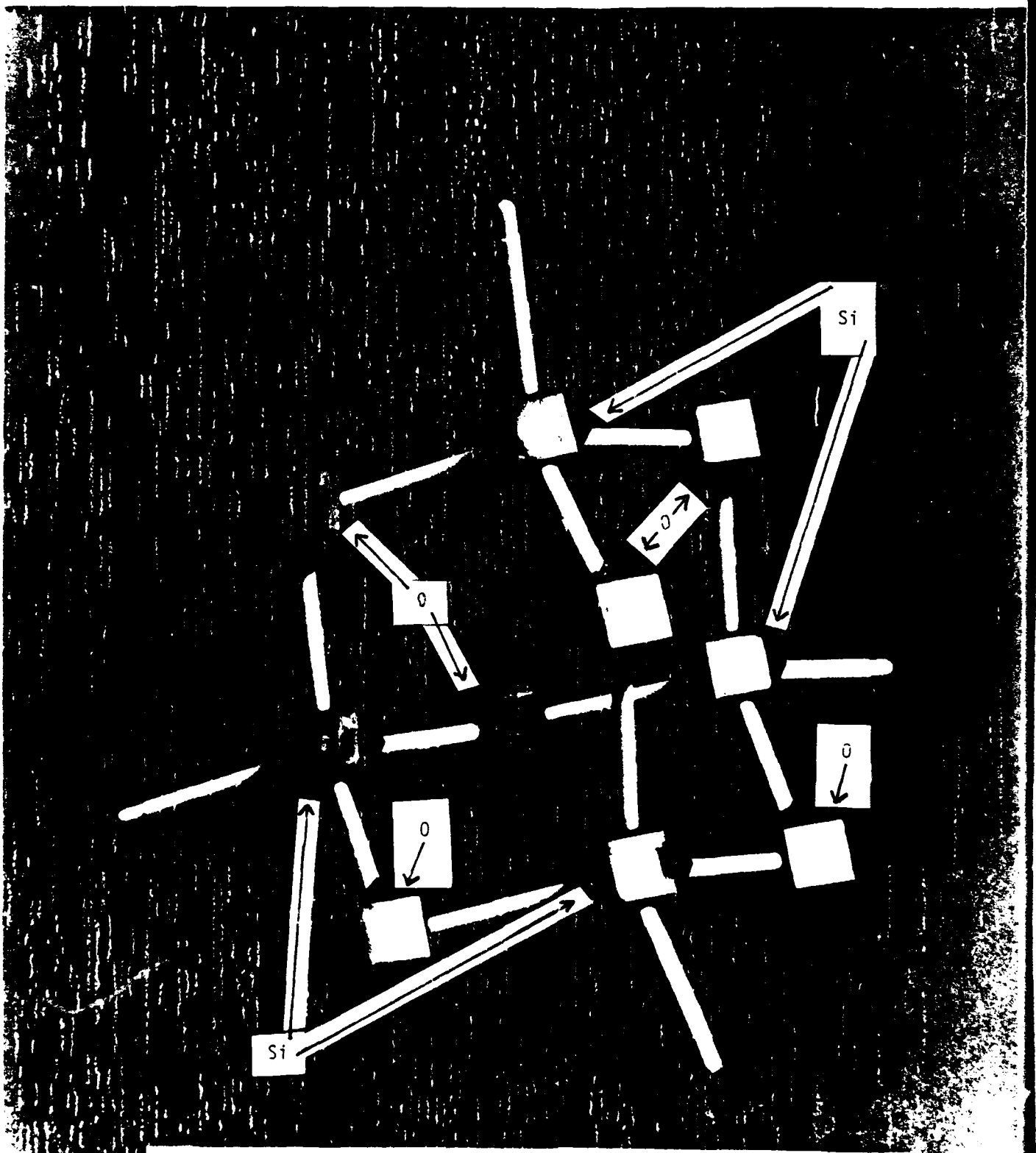

Fig. 16 Si_2O_3 lattice model, seen as Si_4O_6 silicon-like molecule.

Figure 17 shows RED patterns for (100) and (111) single crystal MBE oxides, with (110) incidence for both. The two extra spots between major spots are due to the lattice constant of epitaxial crystalline Si_2O_3, which is three times that of Si, discussed above for Fig. 16. These spots are more pronounced for the (100) wafer because there is no competition from Si_2O. The vertical spacing of the spots (i.e., perpendicular to the dark border) for (111) is very important because it indicates the spacing of Bragg planes in the (111) direction. When the (111) pattern in Fig. 17 is compared with the clean (111) surface in Fig. 8, the vertical spacings in Fig. 8 are found to be 1.31 times larger than those in Fig. 17, while the lateral spacings of major spots on this and other RED patterns appear to be nearly the same. This is, of course, almost exactly what we expect for Si_2O, since the vertical Si-O-Si bond length is known from β-cristobalite to be 1.318 times larger than Si-Si.

These suboxides have caused us enough leakage problems in the MOS experiments that their semiconducting properties may make them inappropriate for MOS applications. They seem to be the single-crystal analog of SIPOS,[6,8] or semi-insulating polysilicon, which is an amorphous mixture including Si_2O and Si_2O_3 that is CVD deposited as a high-bandgap emitter for bipolar transistors. If this single crystal version is suitable as a wide bandgap emitter material (and the failure of ellipsometry at 1.95 eV points to a bandgap in the proper range) when it is doped, then such concepts as I^2L integrated circuits and microwave bipolar transistors with buried wide bandgap emitter layers as discussed by Kroemer[9] and others would be feasible.

A tremendous amount of future work on these crystalline suboxides is possible, since little is known about their bandstructure, electrical properties, optical properties, chemical reactivity, etc. To be sure about the lattice structure and composition, X-ray diffraction and ESCA analysis should be added to additional RED and sputter Auger investi-

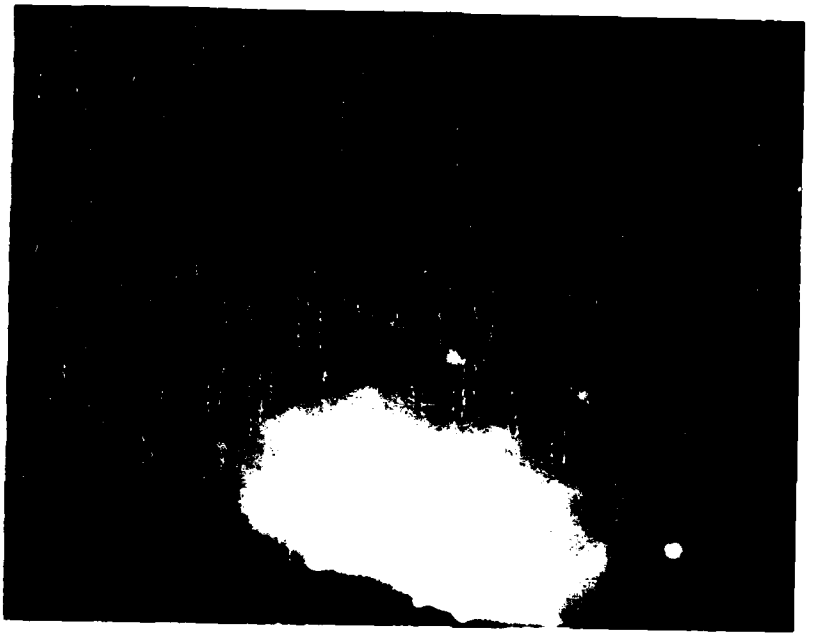

a) (100) Si
with MBE oxide

Fig. 17 RED patterns for a) (100) and b) (111) MBE suboxides.

b) (111) Si
with MBE oxide

gations. The aforementioned photoconductivity experiment can reveal the bandgap, as could a photoluminescence measurement on a thick epitaxial layer. The doping properties and mobility of crystalline Si_2O and Si_2O_3 are of obvious interest, as are their interaction with silicon in various applications (MOS, bipolar, heteroepitaxy, AlGaAs/GaAs-like HEMT devices, etc). All these things can be readily studied at Varian. Bandstructure calculations, lattice mode studies, and interface studies using ultraviolet or X-ray probes are also important, and experiments in other laboratories could benefit from Varian's epitaxial material.

In summary, we believe our initial attempts to oxidize silicon by MBE have resulted, for the first time anywhere, in the formation of single crystal Si_2O and Si_2O_3 suboxides, the former being especially suited to (111) surfaces. These suboxides are largely unstudied, especially in crystalline form. They are grown in vacuum in a narrow temperature range near 670°C by evaporating silicon in the presence of oxygen. Above that temperature, they lose their oxygen and tend to revert back to Si; below it, they grow polycrystalline. At present the bandgap appears to be somewhere between 1.11 and 2 eV. Capacitance-voltage measurements have revealed a dielectric constant between 1.5 and 3, and have shown that the material can accumulate and invert p- and n-type material, although with hysteresis caused by charge injection. Simultaneous conductance-voltage characterization reveals that these suboxides can be conductive, although MIS-type devices and applications are not ruled out. Many possible applications for these compounds are foreseen on account of their wide bandgap and ability to lattice match to silicon.

V. REFERENCES

1. F. Herman, I. P. Batra and R. V. Kasowski, Proc. International Conf. Phys. of SiO_2 and Its Interfaces (1978), p. 333.

2. V. Lappe, IRCON, Inc., private communication.

3. R. C. Henderson, "Silicon Cleaning with Hydrogen Peroxide Solutions: A High Energy Electron Diffraction and Auger Electron Spectroscopy Study", J. Electrochem. Soc. 119, 772 (1972).

4. U. König, H. Kibbel and E. Kasper, "Si MBE: Growth and Sb Doping", J. Vac. Sci. Technol. 16, 985 (1979).

5. M. Wright Jenkins, "A New Preferential Etch for Defects in Silicon Crystals", J. Electrochem. Soc. 124, 757 (1977).

6. J. H. Thomas III and A. M. Goodman, "AES and XPS Studies of Semi-Insulating Polycrystalline Silicon (SIPOS) Layers", J. Electrochem. Soc. 126, 1766 (1979).

7. C. Y. Su, P. R. Skeath, I. Lindau and W. E. Spicer, "Oxidation of Si (111), 7x7 and 2x1: A Comparison", J. Vac. Sci. Tech. 18, 843 (1981).

8. T. Matsushita, N. Oh-uchi, H. Hayashi and H. Yamoto, "A Silicon Heterojunction Transistor", Appl. Phys. Lett. 35, 549 (1979).

9. H. Kroemer, "Heterostructure Bipolar Transistors and Integrated Circuits", Proc. IEEE 70, 13 (1982).